The Journal of Experimental Biology 210, 3728-3735
Published by The Company of Biologists 2007
doi:10.1242/jeb.003251

Light scattering by selected zooplankton from the Gulf of Aqaba

Y. L. Gagnon*, N. Shashar, E. J. Warrant and S. J. Johnsen
Cell and Organism Biology, Zoology Building, Helgonavagen 3, Lund 223 62, Sweden
*Author for correspondence (e-mail: 12.yakir@gmail.com)

Accepted 9 August 2007

Summary

Light scattering by zooplankton was investigated as a major factor undermining transparency camouflage in these pelagic animals. Zooplankton of differing transparencies – including the hyperiid amphipod *Anchylomera blossevillei*, an unknown gammarid amphipod species, the brine shrimp *Artemia salina*, the euphausiid shrimp *Euphausia diomedeae*, the isopod *Gnathia* sp., the copepods *Pontella karachiensis*, *Rhincalanus* sp. and *Sapphirina* sp., the chaetognath *Sagitta elegans* and an enteropneust tornaria larva – were illuminated dorsally with white light (400–700 nm). Spectral measurements of direct transmittance as well as relative scattered radiances at angles of 30°, 90°, 150° and 180° from the light source were taken. The animals sampled had transparencies between 1.5% and 75%. For all species, the highest recorded relative scattered radiance was at 30°, with radiances reaching 38% of the incident radiance for the amphipod *A. blossevillei*. Scattering patterns were also found to be species-specific for most animals. Relative scattered radiances were used to estimate sighting distances at different depths. These calculations predict that all of the examined zooplankton are brighter than the background radiance when viewed horizontally, or from diagonally above or below at shallow depths. Thus, in contrast to greater depths, the best strategy for detecting transparent zooplankton in the epipelagic environment may be to search for them from above while looking diagonally downwards, looking horizontally or looking from below diagonally upwards. Looking directly upwards proved to be more beneficial than the other viewing angles only when the viewed animal was at depths greater than 40 m.

Key words: backscattering, model, sighting distance, transmittance.

Introduction

The open sea is devoid of shelter, making vision an important sense for both predation and predator avoidance (Hamner, 1996; McFall-Ngai, 1990). In this environment, the visibility (or invisibility) of an animal is critical for its survival. Many complex adaptations have developed in response to these unique conditions. Among these are transparency (Chapman, 1976; Johnsen and Widder, 1998; Johnsen and Widder, 1999; Johnsen and Widder, 2001), cryptic coloration (Endler, 1978; Endler, 1990; Endler, 1991; Fuiman and Magurran, 1994; Herring and Roe, 1988; Muntz, 1990), mirrored body surfaces (Denton, 1970), counter shading and counter illumination (Cott, 1940; Denton et al., 1972; Ferguson and Messenger, 1991; Kiltie, 1988; McAllister, 1967), as well as morphological and behavioral adaptations that minimize apparent body or organ size (Seapy and Young, 1986). Further adaptations involve behavior: at least one function of diel vertical migration is to minimize visual predation. It was suggested that animals that have mirrored sides would benefit by orienting their body to or away from the sun to minimize intense light reflections (Johnsen and Sosik, 2003), and cephalopods and heteropods orient their thin intestines into a vertical position regardless of their body's orientation (Seapy and Young, 1986). Counter adaptations for breaking these camouflage strategies include polarization vision, ultraviolet (UV) vision, colored ocular filters and offset visual pigments (Bowmaker and Kunz, 1987; Browman et al., 1994; Loew et al., 1993; Lythgoe, 1984; Muntz, 1990; Waterman, 1981).

Many zooplankton use transparency as their form of camouflage. Since many transparent species have refractive indices close to that of water, relatively little light is backscattered (Johnsen and Widder, 1999). However, the amount of light that the tissue scatters to the sides may be a major factor in its visibility (Chapman, 1976; Johnsen and Widder, 1999). Determining how much this scattered light affects an animal's visibility is not trivial and depends on depth, viewing angle, viewing distance and wavelength (Jerlov, 1976; Johnsen and Sosik, 2003; Kirk, 1986; Kitchen and Zaneveld, 1992; Mobley, 1995).

Although the pelagic light field varies, there are some general constant attributes. Light intensity decreases exponentially with depth, and the spectrum of light narrows, becoming increasingly blue. At depths greater than a few hundred meters the light field becomes cylindrically symmetrical around the vertical axis, regardless of the position of the sun (Jerlov, 1976; Johnsen and Widder, 1998). In contrast, at shallower depths, the light field is generally asymmetric, especially during sunset and sunrise (Jerlov, 1976; Johnsen, 2002).

While much research has examined light scattering from particles and phytoplankton (Ditchburn, 1963), light scattering by zooplanktonic species, and its effect on their visibility, has remained largely unexplored. Some attempts at modeling

visibility have been made previously (Aksnes et al., 1997; Johnsen, 2002; Johnsen, 2003). Most estimated the maximal distance at which a viewed animal can be seen (sighting distance) and subsequently recognized by a viewer. Models have improved with time to include additional parameters, thereby increasing the accuracy of the results (Johnsen, 2002; Johnsen, 2003).

In this study, we investigate light scattered by zooplankton, and its effects on sighting distance. Measurements of the scattered, transmitted and backscattered light were made on individual zooplankton under laboratory conditions. These results were then combined with estimates of radiance at various depths and viewing angles to model sighting distances.

Material and methods

Specimen collection

Specimens of the hyperiid amphipod *Anchylomera blossevillei* Milne-Edwards 1830, an unknown gammarid amphipod, the euphausiid shrimp *Euphausia diomedeae* Ortmann, the isopod *Gnathia* sp., the copepods *Pontella karachiensis* Rehman 1973, *Rhincalanus* sp. and *Sapphirina* sp., the chaetognath *Sagitta elegans* Verrill, and the tornaria larva of an enteropneust, were collected offshore in the Gulf of Aqaba between March 21st and May 20th, 2005, at the Inter University Institute for Marine Sciences in Eilat, Israel. Plankton were collected with a 200 μm plankton-net towed at a depth of 0–1 m during both day and night. Other specimens were collected offshore using a light-trap at night. The light-trap consisted of a lamp next to a suction sampler, which lured and then trapped the animals in a floating netted enclosure, where they remained alive and active until they were gathered the next morning. Specimens of the brine shrimp *A. salina* were obtained from a cultured population at the Red Sea Observatory, Eilat, Israel.

Animals were selected according to size (1–2 mm radius when applicable and equal in size within species, see Table 1), abundance and condition. Rare animals were excluded to avoid low numerical representation, and only healthy looking and actively moving animals were used. The animals' diet was not controlled before collection. After optical testing, most animals were preserved in 3% formalin for later identification and photography. Animal size was analyzed by calculating the area from digital photos using Sigma Scan Pro 5^{TM} software.

Table 1. *Sampled species and the corresponding radius of their image area, as well as methods of collection*

	N	Mean radius (mm)	Capture method
A. salina	5	1.9±0.1	C
E. diomedeae	6	2.9±0.1	L/N
Gammaridae sp.	5	1.0±1.0	L
Gnathia sp.	4	0.9±0.1	L/N
A. blossevillei	6	1.7±0.4	L/N
P. karachiensis	10	1.2±0.2	L
Rhincalanus sp.	2	1.2±0.3	D/L
S. elegans	3	1.9±0.1	D
Sapphirina sp.	5	1.3±0.1	L
tornaria larva (Enteropneusta)	6	1.3±0.1	D/L

Radius values are means ± s.d. of their image area; *N*, number of species collected. C, culture; D, day trolling; L, light trap; N, night trolling.

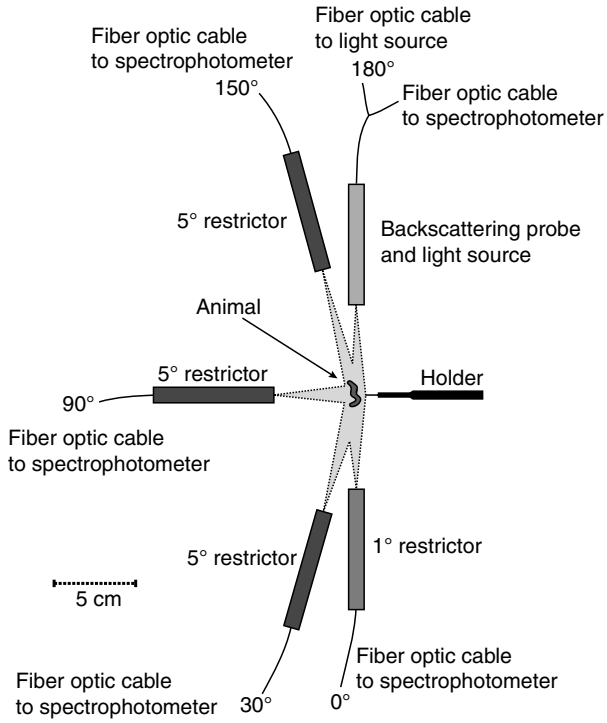

Fig. 1. The apparatus used to measure backscattering, side scattering and transmittance.

Light scattering measurements

Individual animals were glued to the end of a glass pipette (approximately 150 μm thick) with a minute amount of superglue. The pipette was then mounted onto the apparatus holder (Fig. 1), which was submerged in a darkened aquarium filled with seawater (39‰, 20°C) and stationed in a darkroom. All animals were positioned under the light source with their dorsal side upwards. It is imperative to note that some of the variation found in the relative scattering spectra originated from the fact that the animal's dorsal side did not always point exactly towards the light source (zenith).

The apparatus was constructed as follows. An Ocean Optics backscattering probe (model QR400-7-VIS/NIR-BX, Dunedin, FL, USA), which also functioned as the light source, was placed directly over the specimen (viewing angle of 180°). Three fiber optic cables were positioned 12.5 cm from the specimen and at 150°, 90° and 30° from the light source. Each fiber optic cable was covered by a 5° custom-made restrictor made from 7.5 cm long black metal tubes with one end connected to the fiber optic cable and one with a small hole through which light could enter or exit. A fourth fiber optic cable connected to a 1° restrictor (9 cm long) was placed 11.5 cm directly under the specimen (viewing angle of 0°). All optic fibers were 600 μm in diameter. The light source used was an LS-1 Tungsten Halogen lamp (Ocean Optics). A 3-channel cross-calibrated spectrophotometer (Ocean Optics ADC-1000-USB) measured the spectra of the scattered light from 400 to 700 nm. A mirror was placed at 45° underneath the specimen

Table 2. *The scattering angle range for all the sampled animals per viewing angle (i.e. the range of angles deviating from a given scattering angle at which scattered light was still registered for that given scattering angle)*

	Scattering angle range (degrees)				
Species	180	150	90	30	0
A. blossevillei	3.2	4.4	5.2	5.7	9.7
A. salina	3.4	4.8	5.7	6.3	10.6
E. diomedeae	2.6	3	3.6	3.9	6.8
Gammaridae sp.	3.9	6	7	7.8	13
Gnathia sp.	2.2	2.2	2.7	2.9	5.3
P. karachiensis	2.8	3.4	4.1	4.5	7.7
Rhincalanus sp.	4.4	7.3	8.6	9.6	15.8
S. elegans	3.4	4.9	5.8	6.4	10.8
Sapphirina sp.	2.8	3.4	4.1	4.4	7.7
tornaria larva (Enteropneusta)	2.3	2.5	3	3.2	5.8

during backscattering measurements to exclude potential bottom reflection by deflecting the transmitted light sideways onto an immersed black cloth covering the sides of the aquarium. Two of the three spectrophotometer's channels were used interchangeably so as to accommodate all five optic fibers.

This set-up is significantly different from the one previously presented by Johnsen (Farrell et al., 1973; Johnsen and Widder, 1998). In this paper, the light hits the sample at a range of angles depending on the size of the specimen. Since the angular spread of the incident light was 130° in seawater, and since the distance between the light source and the specimen was 14 mm and the width of the light source was 5 mm, samples were struck by light at incident angles ranging from 90° at the centre of the sample to 86° at the edge of the smallest animal (*Gnathia* sp.) or 78° for the largest animal (*E. diomedeae*). It is for this reason that the transparency values calculated in this study are somewhat lower than values achieved with apparatus employing collimated incident light. Furthermore, the acceptance angle for forward scattered light in our apparatus is larger than the standard of 1° (Farrell et al., 1973; Mertens, 1970). The largest angular deviation possible for each viewing angle (i.e. the range of angles deviating from a given scattering angle at which scattered light was still registered for that given scattering angle) is presented in Table 2.

Since the scattering angles inspected in this study differed from each other by 30° or 60°, the large scattering angle range presents little problem. Furthermore, we used relatively small animals in this study (0.9–2.9 mm radius), and the apparatus ensured that whole animals were measured and that examination was not restricted to small sections or tissues of their bodies. In this respect the current set-up better represents biological visual tasks than previous designs (Farrell et al., 1973). This aspect is of special importance when calculating the maximal sighting distance of an animal.

Intensity variations between spectrophotometer-ports and optic fibers were accounted for by measuring white light spectra from all optic fibers and then calculating the ratio of intensities between each optic fiber and the fiber positioned at 0° viewing angle. By multiplying all the outputs from each fiber with that ratio, the variations in intensities were leveled out from fiber to fiber (Sabbah and Shashar, 2006).

The spectral range was limited to 400–700 nm, due to the weak output of the light source at shorter wavelengths and the presumed low visual relevance of underwater infrared radiation.

Relative backscattering, side scattering radiances and transmittance

For each specimen, a series of reference (R), blank (B), dark (D) and sample (S) spectra were taken. The reference spectrum is a measurement of the measured light spectrum at viewing angle 0°, directly underneath the light source, the blank spectrum is taken from the various viewing angles when there is no animal in the apparatus, the dark spectrum is a measurement when there is no light nor animal attached (in all three cases the glass pipette is in place with minute amounts of superglue as control), and the sample spectrum is a measurement when the animal is present. Every measurement is an average value of 3 consecutive measurements of the same sample.

The relative scattered radiance values in this study were calculated as follows. For each viewing angle, the dark spectrum, $D(\alpha)_t$, was subtracted from the spectra obtained from the sample, $S(\alpha)_t$, blank, $B(\alpha)_t$, and reference, $R(\alpha)_t$. Since sample, blank and reference spectra were taken with different integration times, t, dark spectra at each of the integration times were also measured. However, sample and blank spectra all had similar if not equal integration times (7–9 s). Blank spectra were subtracted from the sample spectra and then divided by the reference spectrum. This ratio was then multiplied by the ratio between the solid angle of the light source, Ω_R, as measured from the location of the animal, and the solid angle of the animal, Ω_S, as seen by the fiber optic. Scattering radiance and transmittance were calculated using the following equations:

$$\text{Relative scattering radiance} = \frac{S(\alpha)_t - B(\alpha)_t}{R(0)_t - D_t} \times \frac{\Omega_R}{\Omega_S}, \quad (1)$$

$$\text{Transmittance} = \frac{S(0)_t - D_t}{R(0)_t - D_t} \times \frac{\Omega_R}{\Omega_S}. \quad (2)$$

Transmittance was calculated without a blank, where α was equal to 0°.

Species-dependent scattering

While the relative scattering spectra varied in intensity between all specimens, the shape and form of the sinusoidal spectra (i.e. the relative scattering as a sine function of wavelength) seemed to be similar between specimens within each species. This observation was tested as follows. To exclude variance originating from differences in the magnitude of the relative scattering radiances, each relative scattered radiance spectrum was standardized to a range between –1 and 1. Since each spectrum for each specimen contains more than 600 variables (the spectrophotometer's output for the wavelength span of 400–700 nm), it was necessary to reduce the number of variables that each spectrum possessed. A model (sum of sines; degree=3, see Appendix 1) was fitted to the scaled spectra; the relatively few parameters derived from this model were then applied as variables in the subsequent statistical analysis. Fits with an R^2 value lower than 0.9 were excluded from the

analysis. To balance the dataset to a sample size of 4, groups (i.e. from the same scattering angle and taxonomic group) containing three or less replicates were deleted from the dataset, while excessive replicates (i.e. 5 or more) were randomly erased from the data. To achieve variance homogeneity, data were transformed using a Cox–Box transform (Box and Cox, 1964), which yielded P values larger than 0.3 (Cochran and Bliss, 1970). Homogeneity of covariance was shown using the Box's M test (Winer, 1971). Finally, multivariate analysis of variance (MANOVA) was used on the parameters per scattering angle, to compare the different taxa. The inspected animals were *A. blossevillei* and gammarid amphipods, *A. salina*, *E. diomedeae*, *P. karachiensis*, *Sapphirina* sp., the isopod *Gnathia* sp., and the enteropneust tornaria larva.

Modeling of underwater radiances and sighting distances

Underwater spectral radiance was estimated using the radiative transfer software package Hydrolight 4.1, from Sequoia Scientific Inc. (Bellevue, WA, USA. Using measured inherent optical properties [ac-9 profiles from similar waters (see Johnsen, 2002)], solar elevation and azimuth, atmospheric parameters, sea-surface conditions, chlorophyll fluorescence and Raman scattering by the water, the software computes the radiances as a function of depth, azimuth, wavelength and viewing angle. More detailed information about inherent optical properties (in this case corresponding to Jerlov oceanic water type I) used by the program, and the manner in which it was obtained, is published elsewhere (Johnsen, 2002). The modeled radiances assumed calm seas with light winds, the sun at zenith, and cloudless skies.

A zooplankton's inherent contrast (C_o, contrast at distance zero) is calculated as:

$$C_0(\lambda,z,\alpha) = \frac{L_0(\lambda,z,\alpha) - L_b(\lambda,z,\alpha)}{L_b(\lambda,z,\alpha)}\ , \qquad (3)$$

where L_o is the radiance of the zooplankton and L_b is the radiance of the background, both viewed at a negligible distance from the zooplankton (Hester, 1968; Jerlov, 1976; Mertens, 1970). The variables are wavelength λ (400–700 nm), depth z (0–80 m) and viewing angle α in relation to the nadir (0°, 30°, 90°, 150° and 180°).

Because the downwelling light in our model was several orders of magnitude brighter than light in all other directions, we simplified the calculation assuming it to be the sole illuminant of the target, ignoring contributions from other angles.

The sighting distance (d) is then calculated taking into account the minimum visual contrast threshold of the viewing animal C_{min}, the beam attenuation coefficient c, the attenuation coefficient of the background radiance K_L and the inherent contrast of the viewed animal C_o (Johnsen, 2002):

$$d(\lambda,z,\alpha) = \frac{\ln\left[\left|\frac{C_0(\lambda,z,\alpha)}{C_{min}}\right|\right]}{c(\lambda,z) - K_L(\lambda,z,\alpha)}\ . \qquad (4)$$

The sighting distance is the distance at which an animal of inherent contrast C_o can just be seen by another animal having a visual contrast threshold C_{min}. To incorporate object size as a factor in sighting distance, Johnsen and Sosik used the critical distance after which the viewed animal is too small to be seen as an extended object (Johnsen and Sosik, 2003). The latter depends on the angular spatial resolving power of the viewing animal. Although this parameter is unknown, an angle of 3° was used (Anthony, 1981; Johnsen, 2003). This would mean that the spatial resolution of the viewer (for example an adult Atlantic cod *Gadus morhua*) is such that objects that occupy less than 3° of its visual field are perceived as point sources. When this occurs, the radiance of an object decreases with the inverse square of distance. Detectability can be worked into the model by making the minimum contrast threshold a discontinuous function of the sighting distance:

$$C_{min}(d) = \begin{cases} C_{min} & \text{for } d \leqslant d_c \\ C_{min}\ \dfrac{d^2(\lambda,z,\alpha)}{d_c^2} & \text{for } d > d_c \end{cases}\ , \qquad (5)$$

where C_{min} approximates the minimum object contrast that can

Table 3. *Percent relative scattering radiances, and transmittance (for viewing angle 0°), at wavelength 480 nm with the corresponding standard deviation for the respective viewing angles, where 0° is directly under the specimen*

Species	N	Relative scattered radiance[a] (%) at different viewing angles (degrees)					Transmittance ratio[b]
		180	150	90	30	0	
A. blossevillei	7	0.17±0.11	3.1±1.5	2±1.4	38±8.1	8.4±1.9	0.23
A. salina	6	0.02±0.014	0.4±0.24	0.5±0.34	2.6±1	9.4±2.4	0.38
E. diomedeae	6	0.01±0.015	1.6±0.98	0.92±0.32	4.1±3.3	3.8±0.5	0.2
Gammaridae sp.	5	0.019±0.017	0.76±0.47	0.3±0.41	6.2±2.7	8.0±3.3	0.07
Gnathia sp.	7	0.029±0.024	1.4±1.1	1.5±0.94	10±5	1.4±1.1	0.1
P. karachiensis	11	0.056±0.069	2.3±0.85	1.7±1	6±2.1	4.0±2.1	0.08
Rhincalanus sp.	4	0.048±0.052	2.1±3.5	3±3.8	9±2.2	11.8±3.6	0.17
S. elegans	6	0.0071±0.0067	0.049±0.058	0.073±0.09	0.25±0.35	73.3±7.2	0.03
Sapphirina sp.	6	2.9±3.3	2.5±1.6	3.3±1.9	5.7±3.2	61.0±33.0	0.08
tornaria larva	6	0.039±0.022	1.8±1.2	2.2±1.9	15±6.4	5.6±3.3	0.37

[a]Relative scattered radiance at λ=480 nm.

[b]Transmittance ratio is the slope of transmittance against wavelength divided by transmittance at wavelength 480 nm $[(1/t_{480})\times(dT/d\lambda)]$.

be detected by a given visual system and d_c is the critical distance (Johnsen, 2003). It is also known that minimum contrast thresholds increase with lower light intensities (Douglas and Hawryshyn, 1990; Siriraksophon and Morinaga, 1996), such as those found in deeper waters. This factor was added to the current model by multiplying the original minimum contrast for cod, 0.02 (Anthony and Hawkins, 1983), with the square root of the ratio between the horizontal background radiance at depth zero and 480 nm wavelength and the background radiance at each respective, depth, viewing angle and wavelength. In this manner the minimum contrast threshold was never lower than the original value of 0.02. In a case where the distance from which the animal is viewed is larger than the critical distance, the sighting distance becomes:

$$d(\lambda,z,\alpha) = \frac{\ln\left[\left|\frac{C_0(\lambda,z,\alpha)}{C_{\min}}\right| \times \frac{d_c^2}{d^2(\lambda,z,\alpha)}\right]}{c(\lambda,z) - K_L(\lambda,z,\alpha)} \quad . \qquad (6)$$

This equation has no analytical solution and must therefore be solved by numerical analysis. The preceding method was applied on averaged spectra sampled from each taxonomic group.

Results

Relative backscattering, side scattering radiances and transmittance

The transmittance values, that is the relative spectral radiances at angle 0°, were linearly correlated with wavelength (all R^2 values were larger than 0.93 except for *Gnathia* sp. larvae and gammarid amphipods, where R^2=0.82). Relative scattered radiances, however, were not linearly correlated with wavelength. Relative scattered radiances are shown in Table 3 for a wavelength of 480 nm. The transmittance ratio is the slope of the linear regression normalized by dividing it by the transmittance at 480 nm (Johnsen and Widder, 1998). Transmittance ratios were all significantly different from zero ($P<10^{-7}$), and varied between 0.03 for *S. elegans* and 0.38 for *A. salina*. This ratio is useful because it combines information about the transparency value as well as the variation of transparency values for each wavelength (i.e. color). The latter is important as some visual systems can detect very small color differences, a sensitivity that in vertebrates is often caused by ocular media being more transparent to a certain wavelength than another (Denton and Locket, 1989; Douglas and Thorpe, 1992; Muntz, 1976). Although the ratio is not practical when comparing two animals that differ distinctly in their transparency, it is useful for showing an advantageous lack of coloring when comparing similarly transparent animals.

The most transparent species was *S. elegans* (73.3% at 480 nm), followed closely by *Sapphirina* sp. (61%). Other examined planktonic animals were far less transparent, namely *E. diomedeae* (9%), *A. salina* and *Gnathia* sp. both at 8%, tornaria larva (Enteropneusta) (6%), *P. karachiensis* and Gammaridae sp. (4%) and lastly, *A. blossevillei* with 1%. The transmittance (i.e. viewing angle of 0°) for the averaged results of all the sampled groups is shown in Fig. 2. Note that the transmittance axis is logarithmic.

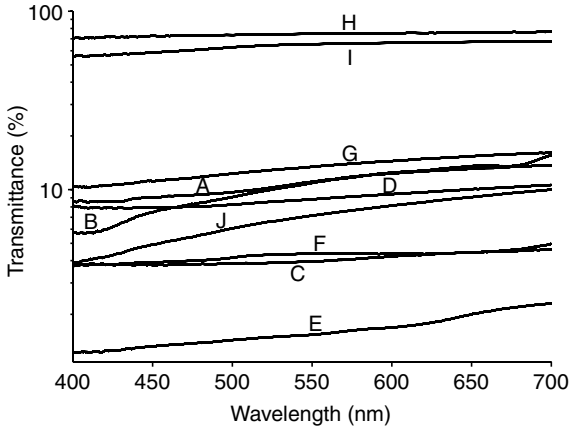

Fig. 2. Averaged transmittances for all the sampled animals. A, *Artemia salina*; B, *E. diomedeae*; C, Gammaridae sp.; D, *Gnathia sp.*; E, *A. blossevillei*; F, *P. karachiensis*; G, *Rhincalanus* sp.; H, *S. elegans*; I, *Sapphirina* sp.; J, tornaria larva (Enteropneusta). Note that the transmittance axis is logarithmic.

For all scattering angles except backscattering, *A. blossevillei* had the largest relative scattered radiances. In *Sapphirina* sp., structural colors caused large fluctuations in the received spectra, leading to large deviations in the results, as well as the largest relative backscattered radiances.

Transmittance and scattering curves for a few representative animals are shown in Fig. 3. The representative animals were chosen based on their transmittance, being either low, medium

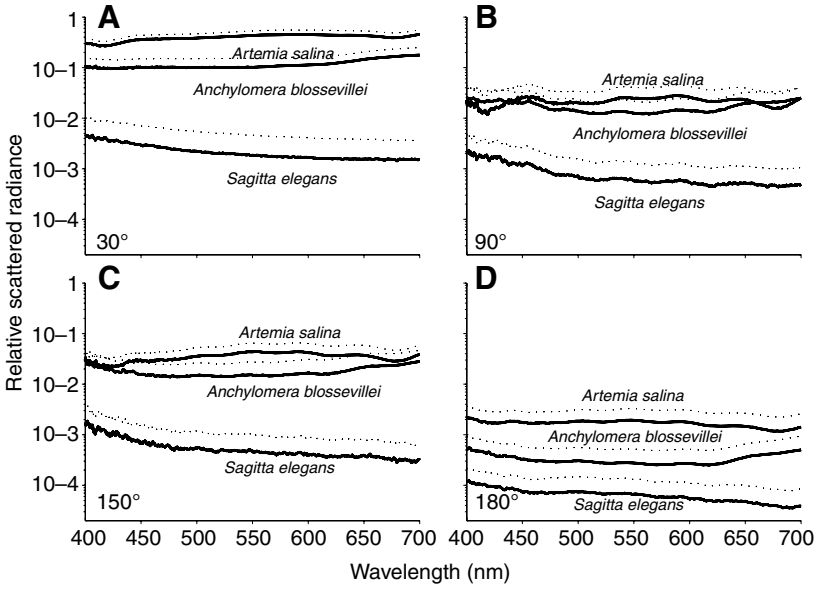

Fig. 3. Relative scattering radiance for (A) 30°, (B) 90°, (C) 150° and (D) 180° (backscattering), for *A. salina*, *S. elegans* and *A. blossevillei*. Dotted lines denote + s.d. Note that radiance axes are logarithmic.

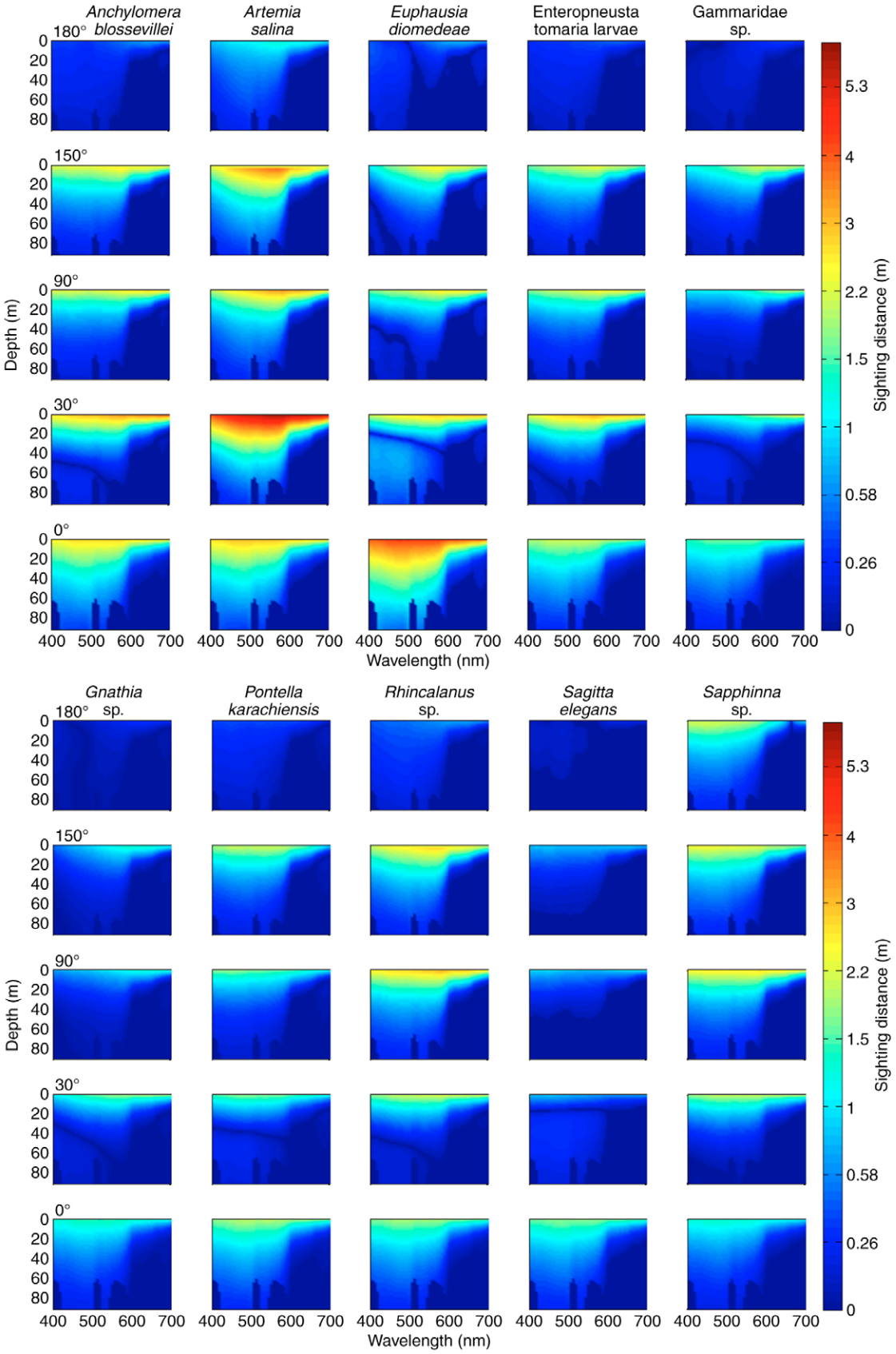

Fig. 4. Sighting distances (m) in all species as a function of wavelength (nm) and depth (m). The sighting distance is color coded in the figures from long distances as red to short distances as blue (see color bar). The following viewing angles (from top to bottom) are displayed: from directly above (180°), diagonally above (150°), horizontal (90°), diagonally below (30°) and directly below (0°).

or highly transparent animals. Relative scattered radiances at 30° ranged from 0.85% to 50% (Fig. 3A). Relative scattering radiances for viewing angles 90° and 150° both range from 0.1% to 4.54% (Fig. 3B,C).

In general, relative side-scattered radiance was always largest at 30° (overall mean 9.7%), while at 90° and 150° lower values were measured (overall mean 1.5% and 1.6%, respectively). Relative backscattered radiance (180°) was the lowest with an overall mean of 0.3%.

A significant difference was found between the species for scattering angles of 30°, 90° and 150° (MANOVA, $P<0.05$), and no significant difference between the species for scattering at 180°. Gammaridae sp., *Sapphirina* sp., *A. blossevillei* and *P. karachiensis* form distinct clusters at scattering angle 90°. Gammaridae sp. had different scattering at 30°. Gammaridae sp. and *P. karachiensis* were different from the other species for a scattering angle of 150°.

Sighting distance

The calculated sighting distance of all sampled animals was generally longer at lower wavelengths and at shallower depths (Fig. 4). Sighting distance was inversely proportional to depth. This is due to the fact that the animal's inherent contrast decreased faster than the water became clearer, as well as the rising minimum contrast threshold with depth. For most animals, sighting distance decreased to zero at a certain depth and increased back to a relatively small distance at deeper waters. This is due to the change of the animals' inherent contrast from positive to negative. In shallow waters, the animals were much brighter than their background, which led to a large sighting distance. As depth increased, their radiance decreased more rapidly than the background radiance, eventually becoming lower than the latter. At a certain depth, the radiance matched the background radiance and the sighting distance dropped to zero.

At a wavelength of 480 nm, *A. salina* had a sighting distance of 5.2 m at a depth of 2 m and a viewing angle of 30°. *A. blossevillei* had a sighting distance of 2.9 m under the same conditions while *S. elegans* had a sighting distance of 0.73 m. The sighting distance was limited for large viewing angles (i.e. 150° and 180°) in shallow depths as these would place the viewing animal out of the water.

Sighting distance was very short for wavelengths longer than 600 nm at depths greater than 20 m. Looking down at the animals (viewing angle 180°) resulted in the shortest sighting distances. This was true for all depths, wavelengths and animals, except *Sapphirina* sp. There was no obvious difference in sighting distance between viewing angles 150°, 90° and 30°. Viewing the animals from directly below resulted in larger sighting distances at depths greater than 40 m for most animals. *E. diomedeae* and *S. elegans* showed to have longer sighting distances at shallower depths as well, while *A. salina* had longer sighting distance at a viewing angle of 30° for most depths.

Discussion

Scattering

The results from the MANOVA indicated that the shape of the relative scattered radiance depended on the species. This in turn suggests that the manner in which zooplankton scatter light is species-specific. That is, the relative scattered radiance *versus* wavelength was found to be relatively uniform within species, but to differ between species. Thus, by using color-dependent light scattering as a signature, each zooplanktonic species can be identified. This chromatic information can be used by predatory animals in search of large congregations of their preferred prey. This feature may also be used to automatically identify and quantify large quantities of zooplanktonic animals in a fast and efficient way.

Sighting distance

An important observation acquired from the sighting distance model is that the object radiance is greater than the respective background radiance at certain viewing angles, and this contributes to the sighting distance pattern seen in Fig. 4. This increased the sighting distance for more dorsal viewing angles despite lower relative scattering values at these angles. Because downward radiance at shallow depths is so much higher than radiance from any other direction, even scattering a small percentage of the former increases the animal's inherent contrast significantly. Inherent contrast, and consequentially sighting distance, reached near-zero values at a depth that depended on viewing angle and wavelength. This dependency was different for each species, differing in depth or wavelength dependency (with *S. elegans* having a virtually zero sighting distance at ~20 m and *Gnathia* sp. from 30 to 70 m). It is possible that animals that want to avoid being seen from those viewing angles may adopt a behavioral strategy of staying at those depth intervals.

These findings suggest that a good strategy for detecting transparent zooplanktonic prey and predators in the epipelagic environment is probably to search for them from above while looking horizontally, diagonally downwards or diagonally upwards. In most cases, detecting the animal's silhouette by looking directly upwards appears to be advantageous at depths greater than 40 m. Some animals were, however, more visible at all depths when viewed directly from below, while a few more were visible at all depths when viewed from 30°.

The short sighting distance seen at longer wavelengths (i.e. >600 nm) depended on the combination of two major factors, minimum contrast threshold and background radiance. The minimum contrast threshold of the viewing animal was inversely proportional to the square root of the background radiance, which decreased extremely rapidly for wavelengths longer than 550 nm. The resulting high contrast threshold at these wavelengths requires large contrast values for the animal to detect the object viewed, which is consistent with the relative rarity of aquatic visual systems that are sensitive to light at wavelength longer than 550 nm (Marshall et al., 1999).

Changes in sighting distance were most dramatic in shallow depths compared with deeper waters, due to the logarithmic manner with which light intensity decreases with increasing depth. Sighting distance did not have any evident correlation with wavelengths between 400 and 600 nm, which is consistent with the high variation in spectral sensitivity found in zooplanktivores (Marshall et al., 1999).

This study shows that zooplanktivores may benefit from looking for their prey at relatively shallow depths diagonally or horizontally to the vertical axis. Such a predation strategy may

be more successful than looking for the zooplankton from directly underneath. Further behavioral studies may support this hypothesis.

Appendix 1

The model used to fit the relative scattering radiance spectra curves is:

$$f(x) = \sum_{i=1}^{3} a_i \times \sin(b_i x + c_i) \ , \qquad \text{(A1)}$$

where x is the wavelength at which each relative scattering radiance value was measured and $f(x)$ denotes the fitted relative scattering radiance. a_i, b_i and c_i are the model parameters.

We thank the staff of the Interuniversity Institute for Marine Sciences, Eilat, and Shai Sabbah for field and laboratory assistance. This study was made possible thanks to financial support from the Royal Physiographic Society in Lund and the Carl Swartz Memorial Fund.

References

Aksnes, D. L., Miller, C. B., Ohman, M. D. and Wood, S. N. (1997). Estimation techniques used in studies of copepod population dynamics – a review of underlying assumptions. *Sarsia* **82**, 279-296.

Anthony, P. D. (1981). Visual contrast thresholds in the cod *Gadus morhua*. *J. Fish Biol.* **19**, 87-104.

Anthony, P. D. and Hawkins, A. D. (1983). Spectral sensitivity of the cod *Gadus morhua*. *Mar. Behav. Physiol.* **10**, 145-166.

Bowmaker, J. K. and Kunz, Y. W. (1987). Uv receptors tetrachromatic color vision and retinal mosaics in the brown trout *Salmo trutta* age-dependent changes. *Vis. Res.* **27**, 2101-2108.

Box, G. E. P. and Cox, D. R. (1964). An analysis of transformations. *J. R. Stat. Soc. Ser. B* **26**, 211-252.

Browman, H. I., Novales-Flamarique, I. and Hawryshyn, C. W. (1994). Ultraviolet photoreception contributes to prey search behaviour in two species of zooplanktivorous fishes. *J. Exp. Biol.* **186**, 187-198.

Chapman, G. (1976). Transparency in organisms. *Experientia* **32**, 123-125.

Cochran, W. G. and Bliss, C. I. (1970). Analysis of variance. In *Statistics in Endocrinology* (ed. J. W. Mcarthur and T. Colton), pp. 33-78. Cambridge, MA: MIT Press.

Cott, H. B. (1940). *Adaptive Colouration in Animals*. London: Meuthen.

Denton, E. J. (1970). On the organization of reflecting surfaces in some marine animals. *Philos. Trans. R. Soc. Lond. B Biol. Sci.* **258**, 286-313.

Denton, E. J. and Locket, N. A. (1989). Possible wavelength discrimination by multibank retinae in deep-sea fishes. *J. Mar. Biol. Assoc. U. K.* **69**, 409-436.

Denton, E. J., Gilpin-Brown, J. B. and Wright, P. G. (1972). The angular distribution of the light produced by some meso pelagic fish in relation to their camouflage. *Proc. R. Soc. Lond. B Biol. Sci.* **182**, 145-158.

Ditchburn, R. W. (1963). *Light*. London: Blackie & Sons.

Douglas, R. H. and Hawryshyn, C. W. (1990). Behavioral studies of fish vision: an analysis of visual capabilities. In *The Visual System of Fish* (ed. R. H. Douglas), pp. 373-418.

Douglas, R. H. and Thorpe, A. (1992). Short-wave absorbing pigments in the ocular lenses of deep-sea teleosts. *J. Mar. Biol. Assoc. U. K.* **72**, 93-112.

Endler, J. A. (1978). A predators view of animal color patterns. *Evol. Biol.* **11**, 319-364.

Endler, J. A. (1990). On the measurement and classification of color in studies of animal color patterns. *Biol. J. Linn. Soc. Lond.* **41**, 315-352.

Endler, J. A. (1991). Variation in the appearance of guppy color patterns to guppies and their predators under different visual conditions. *Vis. Res.* **31**, 587-608.

Farrell, R. A., McCally, R. L. and Tatham, P. E. R. (1973). Wave-length dependencies of light scattering in normal and cold swollen rabbit corneas and their structural implications. *J. Physiol.* **233**, 589-612.

Ferguson, G. P. and Messenger, J. B. (1991). A countershading reflex in cephalopods. *Proc. R. Soc. Lond. B Biol. Sci.* **243**, 63-68.

Fuiman, L. A. and Magurran, A. E. (1994). Development of predator defences in fishes. *Rev. Fish Biol. Fish.* **4**, 145-183.

Hamner, W. M. (1996). Predation, cover, and convergent evolution in epipelagic oceans. In *Zooplankton: Sensory Ecology and Physiology* (ed. P. H. Lenz, D. K. Hartline, J. E. Purcell and D. L. Macmillan), pp. 17-37. Amsterdam: Gordon and Breach.

Herring, P. J. and Roe, H. S. J. (1988). The photoecology of pelagic oceanic decapods. *Symp. Zool. Soc. Lond.* **59**, 263-290.

Hester, F. J. (1968). Visual contrast thresholds of goldfish (*Carassius Auratus*). *Vis. Res.* **8**, 1315-1335.

Jerlov, N. G. (1976). *Marine Optics*. New York: Elsevier.

Johnsen, S. (2002). Cryptic and conspicuous coloration in the pelagic environment. *Proc. R. Soc. Lond. B Biol. Sci. B* **269**, 243-256.

Johnsen, S. (2003). Lifting the cloak of invisibility: the effects of changing optical conditions on pelagic crypsis. *Integr. Comp. Biol.* **43**, 580-590.

Johnsen, S. and Sosik, H. M. (2003). Cryptic coloration and mirrored sides as camouflage strategies in near-surface pelagic habitats: implications for foraging and predator avoidance. *Limnol. Oceanogr.* **48**, 1277-1288.

Johnsen, S. and Widder, E. A. (1998). Transparency and visibility of gelatinous zooplankton from the Northwestern Atlantic and Gulf of Mexico. *Biol. Bull.* **195**, 337-348.

Johnsen, S. and Widder, E. A. (1999). The physical basis of transparency in biological tissue: ultrastructure and the minimization of light scattering. *J. Theor. Biol.* **199**, 181-198.

Johnsen, S. and Widder, E. A. (2001). Ultraviolet absorption in transparent zooplankton and its implications for depth distribution and visual predation. *Mar. Biol.* **138**, 717-730.

Kiltie, R. A. (1988). Countershading universally deceptive or deceptively universal? *Trends Ecol. Evol.* **3**, 21-23.

Kirk, J. T. O. (1986). Light and photosynthesis in aquatic ecosystems. In *Light and Photosynthesis in Aquatic Ecosystems*. Cambridge, New York: Cambridge University Press.

Kitchen, J. C. and Zaneveld, J. R. V. (1992). A three-layered sphere model of the optical properties of phytoplankton. *Limnol. Oceanogr.* **37**, 1680-1690.

Loew, E. R., McFarland, W. N., Mills, E. L. and Hunter, D. (1993). A chromatic action spectrum for planktonic predation by juvenile yellow perch, *Perca flavescens*. *Can. J. Zool.* **71**, 384-386.

Lythgoe, J. N. (1984). Visual pigments and environmental light. *Vis. Res.* **24**, 1539-1550.

Marshall, N. J., Kent, J. and Cronin, T. W. (1999). Visual adaptations in crustaceans: spectral sensitivity in diverse habitats. In *Adaptive Mechanisms in the Ecology of Vision* (ed. S. N. Archer, E. R. L. Djamgoz, J. C. Partridge and S. Vallerga), pp. 285-328. London: Kluwer Academic Publishers.

McAllister, D. E. (1967). The significance of ventral bio luminescence in fishes. *Sci. Rep. Yokosuka City Mus.* **1967**, 5-6.

McFall-Ngai, M. J. (1990). Crypsis in the pelagic environment. *Am. Zool.* **30**, 175-188.

Mertens, L. E. (1970). *In-Water Photography: Theory and Practice*. New York: John Wiley.

Mobley, C. D. (1995). The optical properties of water. In *Handbook of Optics*. Vol. 1 (ed. E. W. Van Stryland, M. Bass, D. R. Williams and W. L. Wolfe), pp. 43.41-43.56. New York: McGraw-Hill.

Muntz, W. R. A. (1976). On yellow lenses in meso pelagic animals. *J. Mar. Biol. Assoc. U. K.* **56**, 963-976.

Muntz, W. R. A. (1990). Stimulus, environment and vision in fishes. In *The Visual System of Fish* (ed. R. H. Douglas and M. B. A. Djamgoz), pp. 491-511. New York: Chapman & Hall.

Sabbah, S. and Shashar, N. (2006). Polarization contrast of zooplankton: a model for polarization-based sighting distance. *Vis. Res.* **46**, 444-456.

Seapy, R. R. and Young, R. E. (1986). Concealment in epipelagic pterotracheid heteropods (Gastropoda) and cranchiid squids (Cephalopoda). *J. Zool. Lond. A* **210**, 137-148.

Siriraksophon, S. and Morinaga, T. (1996). Effect of background brightness on the visual contrast threshold of the Japanese common squid. *Fish. Sci.* **62**, 534-537.

Waterman, T. H. (1981). Polarization sensitivity. In *Handbook of Sensory Physiology*. Vol. 7/6B (ed. H. Autrum), pp. 281-469. New York: Springer.

Winer, B. J. (1971). *Statistical Principles in Experimental Design*. New York: McGraw-Hill.